

<https://doi.org/10.17221/74/2018-SWR>

## Performance analysis of dielectric soil moisture sensor

IFTIKHAR AHMED SAEED<sup>1,a</sup>, MINJUAN WANG<sup>1,a</sup>, YANZHAO REN<sup>1</sup>, QINGLAN SHI<sup>1</sup>, MUHAMMAD HAMMAD MALIK<sup>1</sup>, SHA TAO<sup>1</sup>, QIANG CAI<sup>2</sup>, WANLIN GAO<sup>1\*</sup>

<sup>1</sup>College of Information and Electrical Engineering,  
China Agricultural University, Beijing, P.R. China

<sup>2</sup>Beijing Key Laboratory of Big Data Technology for Food Safety,  
Beijing Technology and Business University, Beijing, P.R. China

\*Corresponding author: [gaowlin@cau.edu.cn](mailto:gaowlin@cau.edu.cn)

**Citation:** Saeed I.A., Wang M., Ren Y., Shi Q., Malik M.H., Tao S., Cai Q., Gao W. (2019): Performance analysis of dielectric soil moisture sensor. *Soil & Water Res.*, 14: 195–199.

**Abstract:** Soil moisture (SM) varies greatly in the soil profile. We developed a low-cost sensor for SM monitoring at three vertical depths. The sensor function was based on dielectric theory to monitor SM. Three linear calibration models were established using different soils. The sensor for each depth showed acceptable statistics of validations. The linear fit coefficient of determination ( $R^2$ ) ranged from 0.95 to 0.99. Root mean square error (RMSE) ranged from 1.35 to 4.30. The sensor performed consistently for at least 4 months, and is suitable for continuous monitoring of *in situ* SM and irrigation scheduling.

**Keywords:** dielectric sensor; soil moisture; vertical depths

Crop yield is highly related to the availability of soil moisture (SM) and it needs to be quantified precisely. SM varies in dry and wet climatic conditions, vegetation cycles, and with soil depths. The continuous estimation of SM at a point scale is challenging, because it changes more dynamically in shallow soils than in subsoils (PENNA *et al.* 2013). Therefore, monitoring of SM in the vertical profile is necessary for understanding the moisture dynamics in soil-plant relationship. Efforts have been made for a long time to determine variables that control the root zone SM, and many automation methods have been described for precise estimation of SM (STACHEDER *et al.* 2009). The indirect methods determine SM using soil dielectric or thermal properties. These include: tensiometers, resistance blocks (CHOW *et al.* 2009), time domain reflectometry (TDR), and frequency domain reflectometry (FDR) (STACHEDER *et al.* 2009). However,

these methods have limitations such as TDR probes are affected by material heterogeneity and electrical conductivity, whilst dielectric probes misinterpret SM, have calibration problems and are unable to measure transient SM, and partitioning gas tracer sensors are slow (STANGL *et al.* 2009; MITTELBACH *et al.* 2012). The other concerns associated with sensors are misapprehension of SM, poor performance with embedded calibration equations, poor measurement of the root zone transient SM, maintenance issues as well as expensiveness (TOPP 2003; MITTELBACH *et al.* 2012). SM estimations on the basis of capacitance are popular due to low cost and accuracy. This study presents a fully automatic high-resolution low-cost sensor which can monitor SM from 3 soil depths with minimum soil disturbance and transmit data

Supported by China Postdoctoral Science Foundation (2018M630222), Project of Scientific Operating Expenses from Ministry of Education of China (2017PT19) and the Open Research Fund of Beijing Key Laboratory of Big Data Technology for Food Safety (BKBD-2016KF08), Beijing Technology and Business University.

<sup>a</sup>These authors contributed equally to this work.

wirelessly. The aims of the study were to (a) evaluate the sensor *in situ*; (b) study the field structural imbalance effect of the continuous SM estimation at specific soil depths on the sensor performance; and (c) integrate the sensor with an irrigation system.

## MATERIAL AND METHODS

The study presents a multiple depth SM monitoring sensor functioning on the dielectric theory, using a signal frequency (TOPP *et al.* 1980). Figure 1 shows the equivalent circuit diagram of the sensor measurement principle. It is a direct current (DC) voltage output sensor which converts voltage into SM. The probe impedance ( $Z_i$ ) is represented as equation (1):

$$Z_i = -j \frac{Z_C}{\sqrt{\epsilon}} \operatorname{ctg} \frac{2\pi\sqrt{\epsilon}}{\lambda_0} L \quad (1)$$

where:

$Z_C$  – probe impedance in the air

$L$  – probe length

$\lambda_0$  – wavelength of a sine wave

$\epsilon$  – soil dielectric constant

$j$  – current density

Then the equation becomes:

$$Z_i = -j \frac{Z_C}{\sqrt{\epsilon}} \operatorname{ctg} \frac{2\pi\sqrt{\epsilon}}{\lambda_0} l = \frac{Z_C}{j\omega\sqrt{\epsilon}} \operatorname{ctg} \frac{2\pi\sqrt{\epsilon}}{\lambda_0} \quad (2)$$

$$Y_L = Z_L^{-1} = \left[ j\omega C_1 + \frac{1}{j\omega L + \frac{1}{j\omega(C_2 + C_x)}} \right]^{-1} = (j\omega)^{-1} \left[ \frac{C_1 + C_2 + C_x - \omega^2 L C_1 (C_2 + C_x)}{1 - \omega^2 L (C_2 + C_x)} \right]^{-1} \quad (3)$$

$$U_i = \frac{Z_L}{R + Z_L} u_i = \frac{\frac{1 - \omega^2 L (C_2 + C_x)}{C_1 + C_2 + C_x - \omega^2 L C_1 (C_2 + C_x)}}{R + \frac{1 - \omega^2 L (C_2 + C_x)}{C_1 + C_2 + C_x - \omega^2 L C_1 (C_2 + C_x)}} u_i = \frac{1 - \omega^2 L (C_2 + C_x)}{R [C_1 + C_2 + C_x - \omega^2 L C_1 (C_2 + C_x)] + [1 - \omega^2 L (C_2 + C_x)]} u_i \quad (4)$$

where:

$\omega$  – angular frequency of electromagnetic waves

$C_1, C_2, C_x$  – capacitance

$U_1, U_2$  – inductor poles

$L$  – voltage

$u_i$  – frequency

$Y_L$  – probe length

$Z_L$  – probe inductance

$R$  – resistance

$$U_2 = \frac{\frac{1}{j\omega(C_2 + C_x)}}{j\omega L + \frac{1}{j\omega(C_2 + C_x)}} U_1 \quad (5)$$

The developed probe is composed of different units including sensing tube, sensor acquisition, processing, frequency oscillation, and wireless communication and power supply. The tube consisted of three moisture sensing rings  $Cx1 \sim Cx3$  and temperature sensitive resistors  $RT1 \sim RT3$ . Figure 2 shows the system block diagram. An application package was developed which was convenient to install, gave consistent SM and temperature measurements, had reliable damp protection and was cost efficient.

Soil samples were taken from three regions of China including a greenhouse, grassland of China Agricultural University (CAU), Beijing, and Yunnan province. These sites had different soil properties and ecological conditions. The textural composition of samples was 60% sand, 10% loam and 30% clay for the greenhouse, 68% sand, 25% loam and 7% clay for CAU grassland and 30% sand, 15% loam, and 55% clay for Yunnan soils. Figure 3 shows the analysis of soil particle size.

The soil samples were homogenized, sieved ( $3 \times 3$  mm) and sterilized at  $30^\circ\text{C}$  for 60 min, and cooled down at room temperature. Three replicates of each sample were prepared in separate buckets. The sensors were installed at depths of 0–15 and 15–30 cm and data were recorded at 15-min intervals. During calibration, the buckets were irrigated several times

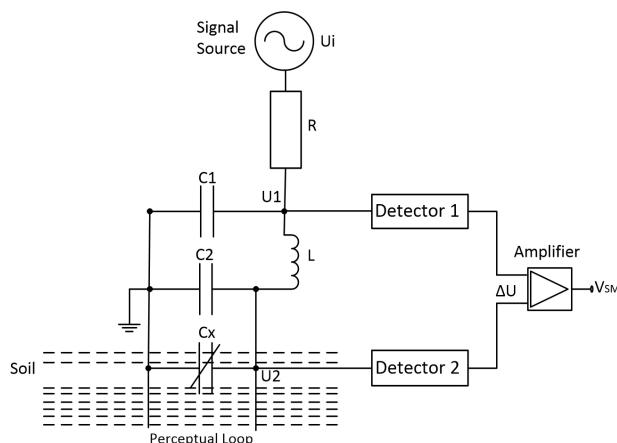


Figure 1. Sensor measurement principle circuit diagram

<https://doi.org/10.17221/74/2018-SWR>

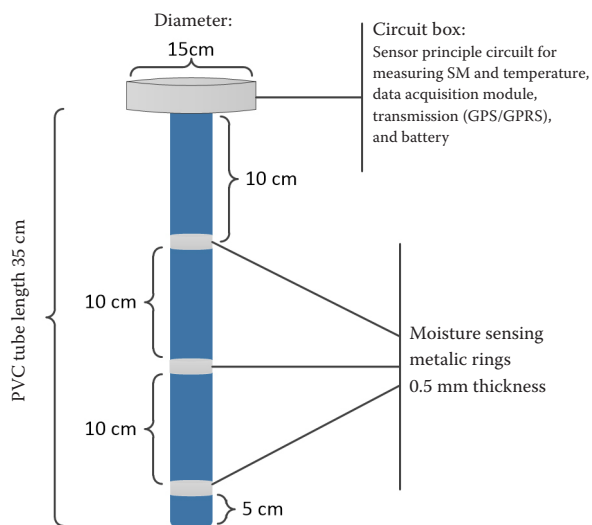


Figure 2. System block diagram

with drip emitters from the top. Samples of sensor adjacent soils were collected and actual SM was measured. The calibration functions were obtained by fitting the estimated and pooled data through linear fit equations and  $R^2$  and RMSE values were calculated. The sensor performance was evaluated *in situ* for measurement consistency, transmission accuracy, power consumption and error rate. A linear multiple depth SM curve was investigated to study a relationship between field structural imbalance and SM. For this, SM from 12 depths, i.e. 10, 15, 20, 25, 30, 35, 40, 45, 50, 55, 60, 65 cm, was measured at 1-h intervals. In the greenhouse where the sensor was installed in November 2017, SM was recorded at 5, 15, and 25-cm depths at a 1-h interval for continuous 600 h. The irrigation tubes were buried at a depth of 15 cm. The irrigation, time, number and water used were recorded.

## RESULTS AND DISCUSSION

The calibration experiments were conducted with three soil samples and pooled data which revealed that the sensor can produce reliable results in different terrains. The sensor measured voltage (mV) and SM linearly fitted results are shown in Figure 4, and the relevant equations in Table 1.

Figure 5 shows the measured SM along with the given irrigation under greenhouse conditions where the sensor captured major SM patterns. The variations in sensor readings with time and at different depths were due to the sensor positioning and irrigation (SOULIS *et al.* 2015).

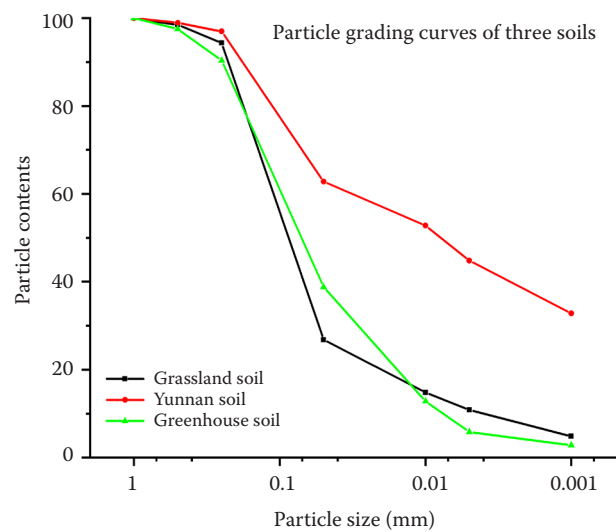


Figure 3. Textural composition of soil samples

The capacitance probes are biased to immediate wet zones, since the electromagnetic field is also influenced by the conductive areas (EVETT *et al.* 2008). The sensor readings at shallow depths were dynamic due to environmental conditions. Furthermore, at depths of 15 and 25 cm, the sensor performance was more stable. Some variations in sensor measurements were due to soil texture because at the same moisture level, the dielectric constant of fine soils is lower than that of the coarse ones (CHENG *et al.* 2013). The sensor performed well at all soil depths and findings were corroborated at all soil depths with time, excluding the irrigation. Similar results have already been reported for loamy and sandy soils while using laboratory calibrated sensors (IRMAK & IRMAK 2005). The sensor error rate was calculated by comparing its observed SM readings with actual SM values. Samples were collected from the greenhouse and SM was measured by oven drying method. In all cases, the error rate was lower than 5%, except the irrigation (12%). Furthermore, the power consumption of the sensor during different modes was calculated as follows: 16.1  $\mu$ A in sleep, 14.8 mA data sensing, 34.6 mA data sending and 14.9 mA data receiving modes. The results

Table 1. Calibration linear fit equations

Linear fit plot	Equation	$R^2$	RMSE
Greenhouse soil	$y = 0.84328 + 24.30639x$	0.958	3.139
Grassland soil	$y = -1.52718 + 23.54394x$	0.959	4.302
Yunnan soil	$y = -3.58187 + 25.93263x$	0.990	2.317
Pooled data	$y = -2.55721 + 25.64864x$	0.995	1.350

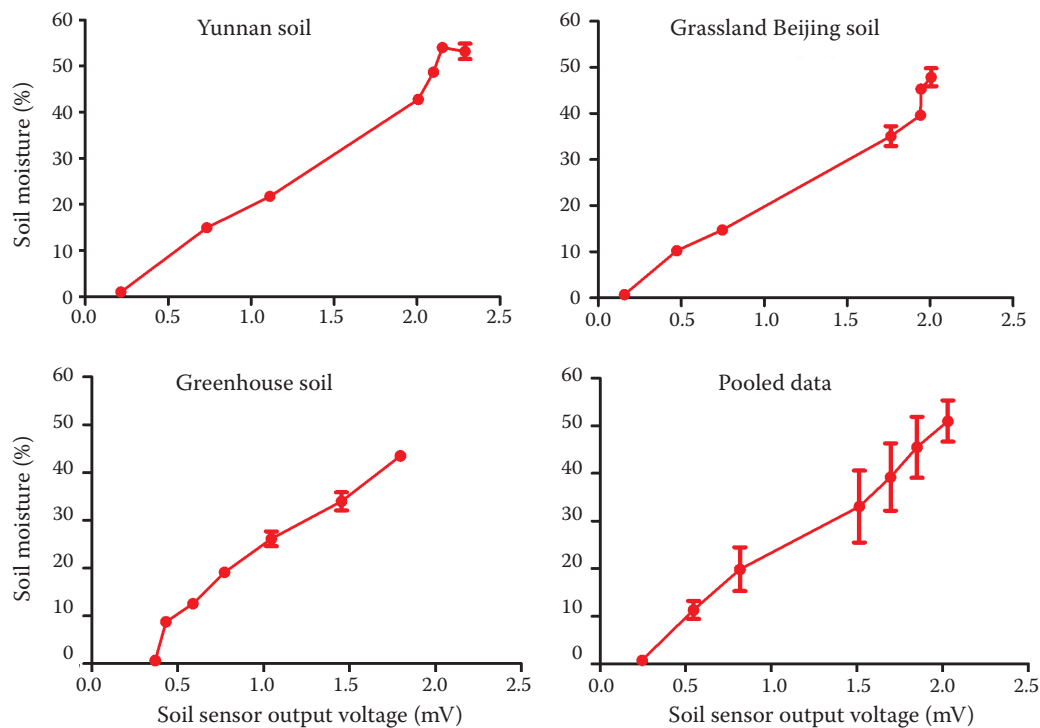


Figure 4. Sensor calibration curves of soil moisture (SM) taken at different locations

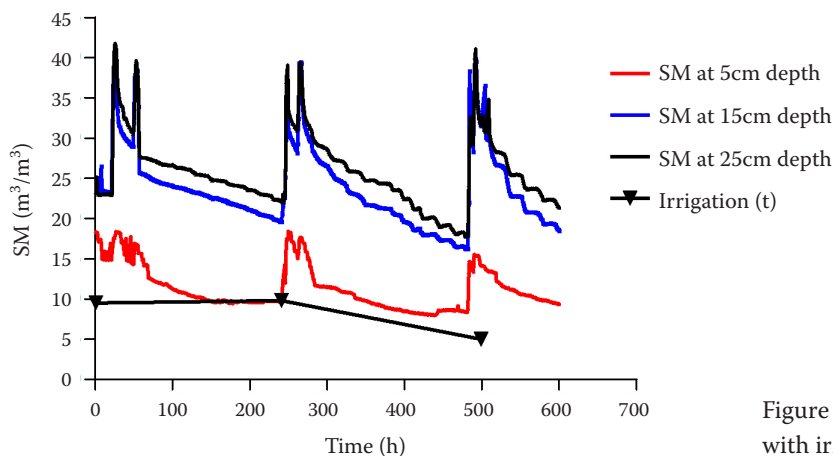


Figure 5. Sensor measured soil moisture (SM) with irrigation in a greenhouse

showed that the sensor accurately estimated *in situ* SM contents and could be used after the irrigation.

## CONCLUSIONS

This study describes SM monitoring sensor based on the dielectric theory. Linear calibration models were established using three different soil samples. An *in situ* SM curve was plotted to study the field structural imbalance effect. The results showed that the sensor can work at least for 4 months with 2100mAh/3.6V battery. Therefore, this new multiple

depth dielectric sensor is very useful for both SM measurements and irrigation planning.

## References

- Cheng Q., Sun Y., Qin Y., Xue X., Cai X., Sheng W., Zhao Y. (2013): In situ measuring soil ice content with a combined use of dielectric tube sensor and neutron moisture meter in a common access tube. *Agricultural and Forest Meteorology*, 171–172: 249–255.
- Chow L., Xing Z., Rees H.W., Meng F., Monteith J., Stevens L. (2009): Field performance of nine soil water con-

<https://doi.org/10.17221/74/2018-SWR>

- tent sensors on a sandy loam soil in new brunswick, maritime region, Canada. *Sensors*, 9: 9398–9413.
- Evelt S., Heng L., Moutonnet P., Nguyen M. (2008): Field Estimation of Soil Water Content: A Practical Guide to Methods, Instrumentation, and Sensor Technology. Vienna, IAEA.
- Irmak S., Irmak A. (2005): Performance of frequency-domain reflectometer, capacitance, and psuedo-transit time-based soil water content probes in four coarse-textured soils. *Applied Engineering in Agriculture*, 21: 999–1008.
- Mittelbach H., Lehner I., Seneviratne S.I. (2012): Comparison of four soil moisture sensor types under field conditions in Switzerland. *Journal of Hydrology*, 430–431: 39–49.
- Penna D., Brocca L., Borga M., Dalla Fontana G. (2013): Soil moisture temporal stability at different depths on two alpine hillslopes during wet and dry periods. *Journal of Hydrology*, 477: 55–71.
- Soulis K.X., Elmaloglou S., Dercas N. (2015): Investigating the effects of soil moisture sensors positioning and accuracy on soil moisture based drip irrigation scheduling systems. *Agricultural Water Management*, 148: 258–268.
- Stacheder M., Koeniger F., Schuhmann R. (2009): New dielectric sensors and sensing techniques for soil and snow moisture measurements. *Sensors*, 9: 2951–2967.
- Stangl R., Buchan G.D., Loiskandl W. (2009): Field use and calibration of a TDR-based probe for monitoring water content in a high-clay landslide soil in Austria. *Geoderma*, 150: 23–31.
- Topp G.C. (2003). State of the art of measuring soil water content. *Hydrological Processes*, 17: 2993–2996.
- Topp G.C., Davis J., Annan A.P. (1980): Electromagnetic determination of soil water content: Measurements in coaxial transmission lines. *Water Resources Research*, 16: 574–582.

Received for publication April 13, 2018

Accepted after corrections December 24, 2018

Published online April 2, 2019